Solar Energy
And Sustainable Development
Refereed, biannual scientific journal issued by
Center for Solar Energy Research and Studies

Aerodynamics Analysis of a Slotted A4412 Wind Turbine Airfoil Using CFD / Case Two

Omar M. Elmosrati*

e-*mail:* [1] *elmosratiomar@yahoo.com*

Abstract: The static pressure, dynamic pressure and velocity magnitude are important parameters and have a strong influence on airfoil lift force. In this paper a slotted NACA4412 airfoil profile is considered for analysis by using the commercial code ANSYS-FLUENT 14.5® at an inlet boundary condition of different approaching wind velocities for various airfoil angles of attack in the range 0˚to 24˚. Renormalized group (RNG) k-ε turbulence model with enhanced wall function is used for the analysis due its' wide usage in the aerodynamic industry. Variations of the physical properties like static pressure, dynamic pressure and velocity magnitude are plotted in form of contours and/or vectors. The main aim of the research is to find out a method to enhance the efficiency of the selected airfoil and its' workability in a wide range of low and high wind speeds which might make it suitable for installation and operation in different climates.

This feasibility of enhancing the lift is and/or minimizing the drag is done by CFD on a series of independently modified NACA4412 airfoils. The current one is called Case 2. The analysis output of Case 2 is not encouraging. It does not show any improvement in NACA4412 airfoil efficiency and therefore it is classified as (obsolete).

التحليل الديناميكا الهوائية لجناح التوربينات الريحية المشقوق CA4412 باستخدام CFD / الحالة 2.

عمر المصراتى

ملخص:

يعد الضغط الساكن والضغط الديناميكي وقيمة السرعة معلمات مهمة ولها تأثير قوي على قوة رفع الجنيح. في هذه الورقة، يتم النظر في ملف تعريف الجنيح المشقوق NACA4412 لتحليله باستخدام الكود التجاري ANSYS-FLUENT 14.5® في حالة حدود المدخل لسرعات الرياح المختلفة التي تقترب من زوايا الهجوم المختلفة للجنيح في النطاق من 0 إلى 24 درجة. يتم استخدام نموذج الاضطراب k-groupالمعاد تشكيله لمجموعة (RNG) مع وظيفة الجدار المحسنة للتحليل نظرًا لاستخدامه الواسع في صناعة الديناميكا الهوائية. تم رسم الاختلافات في الخصائص الفيزيائية مثل الضغط الساكن والضغط الديناميكي وقيمة السرعة في شكل خطوط و/أو ناقلات. الهدف الرئيسي من البحث هو إيجاد طريقة لتحسين كفاءة الجنيح المختار وقدرته على العمل في مجموعة واسعة من سرعات الرياح المنخفضة والعالية والتي قد تجعله مناسبًا للتركيب والتشغيل في المناخات المختلفة.

* *Corresponding author*

هذه الجدوى من تحسين المصعد و/أو تقليل السحب يتم عن طريق CFD على سلسلة من الجنيحات NACA4412 المعدلة بشكل مستقل. الحالة الحالية تسمى الحالة 2. إن نتائج تحليل الحالة 2 ليست مشجعة. لا يظهر أي تحسن في كفاءة الجنيح NACA4412 وبالتالي يصنف على أنه (قديم)..

Keywords: *CFD, NACA4412, wind velocity, wind turbine, Slot, efficiency enhancement HAWT, performance improvement, Aerodynamic optimization, Ansys-Fluent, k-ε model.*

1. INTRODUCTION

Due to the increase of the world concerns over energy security, greenhouse gases, lack of energy sources and environmental pollution; the researchers take an ambitious and practical steps in developing renewable and environmentally friendly energy sources such as wind, solar, hydro-power, geothermal, hydrogen, and biomass as the replacements for the traditional depleting energy source like fossil fuel.

Wind energy can provide suitable solution to global energy security with a maximum consideration to the environment. Wind power is one of the most important sources of renewable energy and it is expected to take a much higher portion in power generation in the coming decades due to the wide availability of the wind and the economic aspect of its design. The European Wind Energy Association (EWEA) declared, "Between 2011 and 2020, the annual onshore market for wind turbines will grow steadily from around 7 GW per year to around 10 GW per year. The offshore market will increase from 1.2 GW in 2011 to reach 6.8 GW in 2020 ((EWEA), 2009)"[1].

"Wind energy is the largest source of added renewable energy generation in the United States since 2000. A plan has been set by the program for 20% of the nation's electricity to be supplied by wind by the year 2030, and 35% by 2050. The report states that a key to achieving this goal is to improve the potential of low-wind-speed locales. Because of this, many works are underway involving the efficiency of wind energy conversion systems, especially for regions with low average wind velocities (Salyers, Travis E., 2016)"[2]

The power generated from the wind is mainly dependent on the aerodynamic performance of the wind turbines. This includes the forces generated by the individual blades, the interactions between them in a rotating configuration, the effects of the turbine's structure and the area terrain. The problem of boundary layer separation from the airfoil surface and the formation of wake(s) is/are also an important subject of study to designers and researchers due to its' direct effect on the airfoil performance specially in the regions of low wind speed which is the case in the widest area of the Libyan country peninsula .

Wind turbines are designed and fabricated based on different classifications. One classification is based on the orientation of the rotor as either Vertical Axis Wind Turbine (VAWT) or Horizontal Axis Wind Turbine (HAWT). HAWT is the type that covered in this paper.

"Over the years, wind turbine blades has gone through many phases of development, researchers are still trying to improve the performance of the wind turbine "Rohan Kapdi, Rahul Dahiya and Vishal Gangadhar Naranje, , 2016" [3]. Some researchers worked on the HAWT performance enhancement on different airfoils types by using different methods than the method used in this paper according to references (4, 5). S.Beyhagi and R.S.Amano[6] made an enhancement trail of NACA4412 efficiency by drilling two segment slots narrow that allow some of the incoming air to flow through them and then exit from the bottom surface of the airfoil span-wide channels near the leading edge. They claimed that (an average improvement of 8% is observed for lift coefficient over the entire range of AoA).

2-PROBLEM STATEMENT & THE AUTHOR PREVIOUS WORK ON THE SUBJECT

The problem of turbulent boundary layer separation from the airfoil surface and the formation of wake(s) is an important subject of study to designers and researchers due to its' direct effect on the airfoil performance.

In order to maximize the wind turbine efficiency; researchers carry out experimental and data analysis of the turbine blade and its surround environment and / or structure by using suitable wind tunnel for testing and theoretical studies. These efforts require expensive laboratory equipment beside they are time consuming. Alternatively, in recent times- the researchers can use the simulation through the Computational Fluid Dynamics (CFD) software that offers a handy solution to the aerodynamic analysis problem.

The author used ANSYS-FLUENT 14.5 Software to make the aerodynamic analysis of NACA4412 airfoil shown by Figure (1) in a two-dimensional (2D) plane after had been modified by incorporating a different slot each time on its' structure. Every modification is completely considered as an independent case by itself and it is analyzed at a different wind speeds by the application of a properly fast and suitable computer. The simulation output of the different physical parameters are plotted and analyzed. The main aim is to find out the effect of slots on the airfoil performance (lift, stall angle, cut-in speed…..).

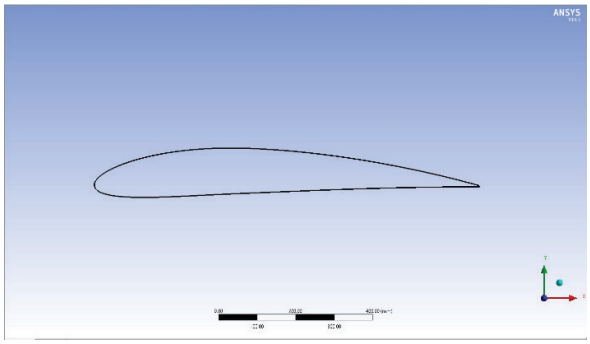

Figure 1. Typical NACA 4412 [7]

3-METHODOLOGY AND VALIDATION

1. The author used the technical paper published by Saxena & Agrawal(8) in order to make a back-to-back validation of the required input physical parameters to the software Fluent®. A comparison of the output results of both Saxena & Agrawal and the author for the velocity magnitude contours of NACA4412 at AoA15 is shown by Figures (2) & (3) and table (I). It is worth noticing that (81%) of the values have a complete match while there is only (0.1%) deviation in the remaining values.

2. The validated physical parameters with the proper number of converged mesh cells were applied to the Software and used in the modeling and simulation of the slotted NACA4412 airfoil that is named Case (2) and shown by Figure (5).

3. The output of the modified NACA4412 airfoil (i.e Case 2) is evaluated against the non-modified NACA4412 at different angles of attack for performance comparison.

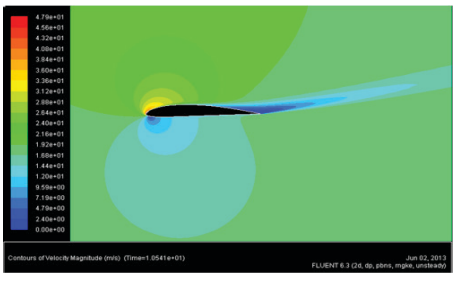

Figure 2. Velocity Magnitude Contours at AoA15 and V=18.4 m/s [8].

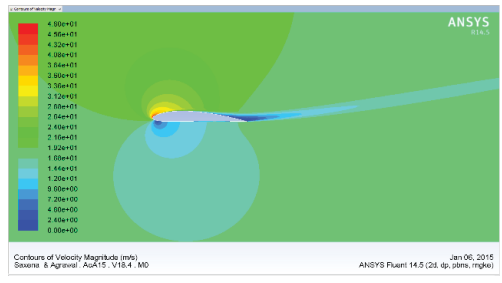

Figure 3. Velocity Magnitude Contours at AoA15 and V=18.4 m/s [7]

Table I: Percentage change of velocity values as calculated in Figs. 2 & 3

Title/No.	1	2	3	4	5	6	7	8	9	10	11	12	13	14	15	16	17	18	19	20	21
Saxena & Agrawal Technical Paper	47.90	45.60	43.20	40.80	38.40	36.00	33.60	31.20	28.80	26.40	24.00	21.60	19.20	16.80	14.40	12.00	9.59	7.19	4.79	2.40	0.00
Validation	48.00	45.60	43.20	40.80	38.40	36.00	33.60	31.20	28.80	26.40	24.00	21.60	19.20	16.80	14.40	12.00	9.59	7.19	4.79	2.40	0.00
% Change	0.2088	0.00	0.00	0.00	0.00	0.00	0.00	0.00	0.00	0.00	0.00	0.00	0.00	0.00	0.00	0.00	0.1043	0.1391	0.2088	0.00	0.00

4-SUMMARY OF THE AUTHOR PREVIOUS WORK ON THE SUBJECT

Case One[9] – This case was discussed in an independent published paper - covered the connection of NACA4412 airfoil both sides. The slot starts from the airfoil pressure side (at 11.5% of the chord length) and extends toward the airfoil suction side in a curved shape side (at 20% of the chord length). Both groove edges at the inlet (at the pressure side) and outlet (at the groove suction side) remain sharp as shown by Figure (4).

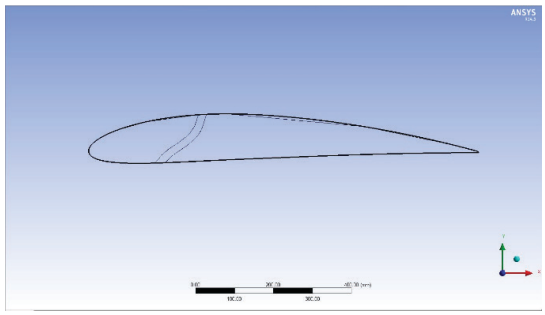

a)- Case One geometry

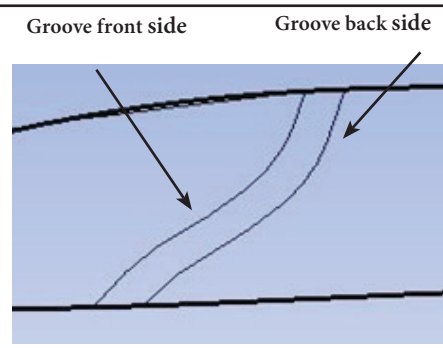

b)- Magnified groove area

Figure 4. Case One airfoil Geometry

Case 1 showed that the slot has a bad impact on the lift due to the build-up of the static pressure on the trailing edge upper side behind the slot due to the flow separation. This had been occurred at all angles of attack and wind velocities except when (AoA0) and wind velocity is 0.3 m/s.

5- CASE TWO GENERAL DESCRIPTION

In this paper, the original standard airfoil NACA4412 shown in Figure (1) was modified by making a groove that starts from the suction side at about 73.5% of the chord length and extends downwards toward the pressure side to cross it at about 76% of the chord length forming two curved surfaces and forms a sharp sides with both pressure and suction sides.

This case was named as **Case Two**.

6-NUMERICAL MODEL

Case Two was solved by using RNG K- ε turbulent model[10] equations with the enhanced wall function where a C-type computational simulation domain (virtual wind tunnel) is used. The domain inlet extends about (12.5c) from the airfoil leading edge side towards the negative x-direction to form the domain inlet (upstream side) and by 21c from the trailing edge side towards the positive x-direction to form the domain outlet (downstream side). The domain height is around (28c) divide symmetrically between both the pressure side and the suction side of the airfoil, as shown by Figure (6). The airflow stream with different velocities is

considered at the inlet of the domain while the model is bounded by wall at the pressure side and the suction side in the domain.

The model equations[11] -which available in different turbulent books- are summarized as:

$$\frac{\partial}{\partial t}(\rho k)+\frac{\partial}{\partial x_i}(\rho k u_i)=\frac{\partial}{\partial x_j}\left[\left(\mu+\frac{\mu_t}{\sigma k}\right)\frac{\partial k}{\partial x_j}\right]+G_k+G_b-\rho\varepsilon$$

The equation of the turbulent kinetic energy K:

The equation of the dissipation rate of the turbulent kinetic energy

$$\frac{\partial}{\partial t}(\rho\varepsilon)+\frac{\partial}{\partial x_j}(\rho\varepsilon u_j)=\frac{\partial}{\partial x_j}\left[\left(\mu+\frac{\mu_t}{\sigma_\varepsilon}\right)\frac{\partial \varepsilon}{\partial x_j}\right]+\rho C_1 S\varepsilon-\rho C_2\frac{\varepsilon^2}{k+\sqrt{\upsilon\varepsilon}}+C_{1\varepsilon}\frac{\varepsilon}{k}C_{3\varepsilon}G_b$$

Where: $\mu_t=\rho C_\mu\frac{k^2}{\varepsilon}$

G_k: Generation of turbulence kinetic energy due to the mean velocity gradient

G_b :Generation of turbulence kinetic energy due to buoyancy

u_(i,j):is the time-averged fluid velocities in the ith and jth directions respectively

K: Turbulent kinetic energy

C_μ:Function of gradient velocity

ε:Dissipatin rate of turbulent kinetic energy

C_1,C_2, C_1ε and C_3ε are constants,

σ_k and σ_ε are turbulent Prandtl numbers for k and ε respectively

ρ:Liquid density

μ:Molecular viscosity of liquid

μ_t:Turbulent viscosity

i,j,k denote the three directions in the global Cartesian system

The model constants are C_1ε=1.44,C_2=1.9,σ_k=1.0, σ_ε=1.2

The model equations are solved numerically with the consideration of the following:

- Fluid physical properties are (fluid type: air, pressure: 101,325Pa, kinematic viscosity: 1.2800E-05 m^2/s).
- Pressure based close out model was selected.
- Monitoring accuracy is set at (1.0e-06) for all parameters.
- The overall domain was divided into blocks in which the quadrilaterals structured mesh with a more than three million converged cells was applied.
- The mesh at the boundary layer area was refined in order to be capable to catch as much as possible the variations in the flow physical parameters.
- The chord length is 1m.
- The boundaries of the domain are set at as; the inlet is set as a flow velocity (m/s), the outlet as a vent to the outside atmospheric pressure and the surfaces of the airfoil are set to wall.

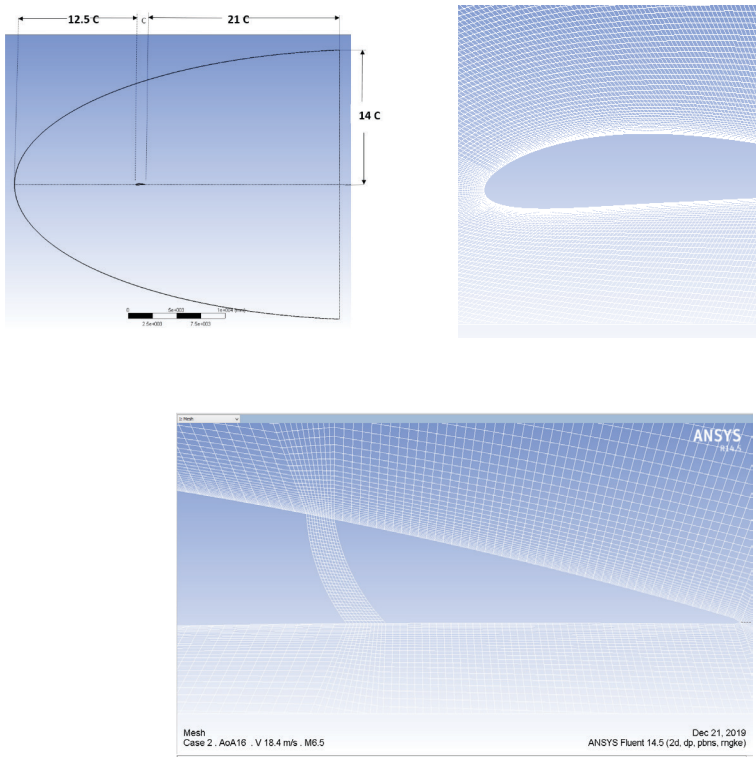

Figure 6. Case Two simulation domain & Mesh

7-CASE TWO OUTPUT RESULTS

This case was computed at the following velocities and angles of attack shown by the table (II) below:

Table II: Simulation points

Approaching wind velocity (m/s)	Mach Number	AoA(deg)
0.3	0.0009	0, 5
2	0.0059	0, 5
3.4	0.01	0, 5
5.5	0.0162	0, 5
18.4	0.0541	0, 5, 10, 16, 17, 18, 20, 21, 22, 23, 24, 25, 26

7.1-Stall Angle

Case Two showed a change of the stall angle of the attack from (20˚) which recorded by the original NACA 4412 airfoil to (22˚) in this case, also recorded a lift force of (407.55015 N/m) at this angle in comparison with the NACA 4412 airfoil lift force of (448.11421 N/m) which gives a decrease of (-9.052%) in the lift force value at this angle, as shown by Figure (7). The calculation was performed according to (Munson et al, 2009) referred to in reference (12). The following analysis is for a selected simulation scenario for different angles of attack and approaching wind velocities.

7.2-Velocity Magnitude

When the approaching wind velocity is 18.4 m/s and AoA22, the velocity magnitude at the airfoil pressure side is (60 m/s) and it decreases gradually to around (0 m/s) at (8%) of airfoil chord line where the flow separated from the surface. The velocity starts increasing gradually up to (12.5 m/s) at the airfoil groove backside edge and continues doing so until it reaches (18 m/s) at airfoil trailing edge (at 100% of the chord line length).

On the suction side, the velocity magnitude value is (60 m/s) at the leading edge of the airfoil; then it decreases sharply to (13 m/s) within a distance equals to (3.5%) of the chord length, then it starts decreasing gradually to reach the (0 m/s) at (49%) of the airfoil chord length where flow separation. The flow remain at around a velocity envelope of (2.5 m/s) after separation until about (99%) of the airfoil chord length where the velocity magnitude increased sharply to reach (7.5 m/s). The velocity of the flow inside the groove recorded (6 m/s) on the groove front side (leading edge side) and recorded the maximum value on the other side of the groove (trailing edge side) where it recorded a value of (23 m/s) as shown by Figure (9). The wall shear stresses shown by Figure (10) and the increase of the angle of attack helps the formation of adverse pressure gradient which leads to the formation of fluid turbulent back flow, and as a result of the interaction between the flow streams vortices are formed. The vortices has a direct impact on drag force increase, as shown by Figure (14) and represented graphically by Figures (11-13).

When the flow behavior is analyzed at approaching wind velocity of 18.4 m/s with AoA16; the slot is also plays the major role in the formation of heavy turbulences in a shape of wakes both inside the slot itself and on the trailing edge suction side which clearly seen by Figures (15, 16).

The Reynolds number, which is used for fluid flow classification to be either laminar flow or turbulent flow, is developed by the laboratory experimental observation work. Based on this, and as shown by Figure (17) the flow over the suction side is (laminar separated periodic flow) in the range from the leading edge up to 0.05m then the flow is changed to (laminar separated steady flow) up to a small distance before the slot where it changed to (laminar separated attached flow). After the flow passed the slot it started to change gradually again to (laminar separated steady flow) up to the trailing edge. Similarly, the flow at the pressure side of the airfoil started as (laminar separated periodic flow) for a length of 0.01m from the leading edge, the flow then starts to change to (laminar separated steady flow) up to point of 0.04m from the leading edge then changed to (laminar separated attached flow) for a short time then the flow changed to (laminar separated steady flow) up to the trailing edge. The flow inside the slot is a (laminar separated periodic flow). The flow immediately changed to (periodic turbulent wake) after it passes the trailing edge as shown by the Figure (17), turbulent kinetic energy shows clearly the contours of the flow and the formation of wakes which has a negative impact on the lift force; as shown by Figure (18).

"The sum of static and dynamic pressure is the total pressure and its difference on the upper and lower surface is the cause of the lift (Prabhakar, 2013)"[13]. The approaching flow splits at the airfoil stagnation point on the leading edge into two streams; first stream travels towards the airfoil upper surface while the other one travels towards the lower one. According to Bernoulli equation, the static pressure will be at its maximum value at the stagnation point where the approaching fluid velocity is zero. Both static and total pressure of case 2 is badly effected due to the presence of the slot; this is expressed in a form of wakes formation and lift/drag force ratio decrease, this is shown by Figures (8, 19, and 20).

Since Case 2 gives a lower lift force than NACA 4412 at approaching wind velocity of (18.4 m/s) as shown by the above analysis and table (III), Then this case is not suitable at high wind velocities.

For the low wind velocities in the range of (0.3-5.5 m/s) on Beaufort wind speed scale (Article, 2015) [14] and at the small airfoil angle of attacks in the range AoA0 & AoA5; Case 2 has a lower lift force than the non-modified airfoil case of NACA 4412 for all studied low wind velocities as shown by table (IV). The reason behind that is the formation of vortices inside the slot and the beginning of the flow separation at the trailing edge suction side where the negative pressure gradient leads to the formation of backward flow and consequently increases the drag force, as shown by Figure (21-25).

Table (III): Variation of Lift Force (N/m) of Case Two with respect to NACA4412 at different airfoil angles of attack and approaching wind speed of 18.4 m/s.

Case \ AoA	AoA0	AoA5	AoA10	AoA16	AoA17	AoA18	AoA19	AoA20	AoA21	AoA22	AoA23	AoA24
NACA 4412	105.8	224.36	330.48	421.92	429.6	433.64	433.13	448.11	437.75	440.59	439.23	422.42
Case 2	65.358	168.09	258.7	356.05	369.13	382.14	390.53	399.87	406.89	407.55	404.07	398.93
% of Variation	-38.23	-25.08	-21.72	-15.61	-14.07	-11.88	-9.836	-10.77	-7.05	-7.499	-8.004	-5.561

Consequently Case 2 is not applicable at all low angles of attack rang at low approaching wind speeds.

Table (IV): Variation of Lift Force of Case Two with respect to NACA4412 at low angles of attack and low wind speed

AoA \ Wind Velocity	0.3 m/s	2 m/s	3.4 m/s	5.5 m/s
AoA0	-110.349%	-39.242%	-37.739%	-39.082%
AoA5	-59.591%	-23.891%	-23.291%	-24.798%

The coefficients of lift and drag at the converged iterations at the AoA16 and approaching wind velocity of 18.5 m/s is shown by table (V). The table shows a considerable reduction of (C_L) despite (C_D) shows a higher reduction value.

Table (V): Variation of C_L and C_D of Case 2 Two with respect to NACA4412 at AoA16 and V 18.4 m/s

	C_L	C_D
NACA4412	1.7586	0.46105
Case 2	1.491	0.3653
% Change	-15.22%	-20.7678%

8-CONCLUSIONS

Comparison of the modified NACA 4412 (i.e Case 2) characteristics with the original NACA 4412 airfoil; the following can be concluded:

1. Case 2 does not show any improvement in the lift force in the low wind velocities range of (0.3-5.5 m/s) according to Beaufort scale, furthermore; the drag force increased tremendously.
2. Case 2 does not show any improvement in the lift force at approaching wind velocity of (18.4 m/s) at all airfoil angles of attack in the range (AoA0-AoA22).
3. **Case 2 has a lower (lift/drag) ratio than NACA 4412 at all angles of attack greater less than 22.5˚at high approaching wind velocities, but after this angle the drag force stars decreasing while lift force starts increasing.**
4. **Case 2 recorded a new critical angle of attack of (22˚) in comparison with NACA 4412 which has critical angle of attack of (20˚) but recorded a lower lift force by a percentage of (-9.052%) comparing with NACA 4412 critical angle of attack lift force.**
5. **Case 2 is proved a useless case because it does not show any enhancement in efficiency better than the original NACA4412.**

6. **It is recommended that the slot be placed horizontally starting from the leading edge side of the aerofoil.**

9-REFERENCES

[7]. European Wind energy Association (EWEA). (2009). Wind Energy- The Facts. London-Sterling, VA: Earthscan.ISBN 978-84407-710-6

[8]. Salyers, Travis E. (2016). "Experimental and Numerical Investigation of Aerodynamic Performance for Vertical-Axis Wind Turbine Models with Various Blade Designs ". Electronic Thesis Dissertations. 1418.

[9]. Rohan Kapdi, Rahul Dahiya and Vishal Gangadhar Naranje. (2016). "Analysis and Optimization of Horizontal Axis Wind Turbine Blade Profile", IJRET, Volume (05); Issue (07). .

[10]. Farha khanamm Neelesh Soni, "Performance Improvement of Horizontal Axis Wind Turbine by Using Modified Blade of NACA 5510", Feb.2016,IJARSET,Vol.3 Issue 2.

[11]. Shafiqur Rehman et el, "Horizontal Axis Wind Turbine Blade Design Methodologies for Rfficiency Enhancement- A Review", energies 1018, 11, 506.

[12]. S.Beyhagi and R.S.Amano "Improvement of Aerodynamic Performance of Cambered Airfoils Using Leading-Edge Slots", Journal of Energy Resources Technology, 2017, Vol.139 / 051204-1

[13]. Omar M. Elmosrati, "Effect of Perforated Leading Edge on Aerodynamics Behavior of Wind Turbine Blades", 2015, Ph.D. Thesis.

[14]. Mahendra Agrawal and Gaurav Saxena "Aerodynamic Analysis of NACA 4412 Airfoil Using CFD", 2013, IJETE, Vol.4, ISSN 2249-6149.

[15]. Omar M. Elmosrati, Maher G. Higazy, Muhamed A. Moawed, Ashraf A. Lashin "Aerodynamics Analysis of a Slotted NACA4412 Wind Turbine Airfoil Leading Edge Using CFD Case One",2015, ERJ, Volume(26).

[16]. D.C.Wilcox "Turbulent Modeling for CFD",DCW Industries, Inc., 1993, ISBN:0-9636051-0-0.

[17]. Igor V.Minin, Oleg V.Minin: "Computational Fluid Dynamics Technologies and Applications", 2011, InTech, ISBN:978-953-307-169-5

[18]. Munson et al.,"fundamentals of fluid mechanics",Wiley, 2009, ISBN: 978-0470-26284-9.

[19]. Arvind Prabhakar; "CFD analysis of static pressure and dynamic pressure for NACA 4412", 2013, IJETT, Volume4; issue8, ISSN: 2231-5381.

[20]. http://www.actionsportsmaui.com/asm_beahfort_scale.html?gclid-CNaonNuxsMCFUHmwgod2SMAqg as on 03.Feb.2015

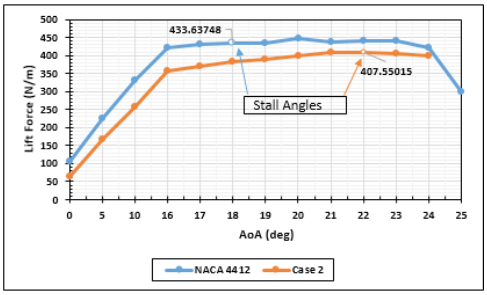

Figure 7: Comparison of lift force and AoA between Case Two and NACA 4412

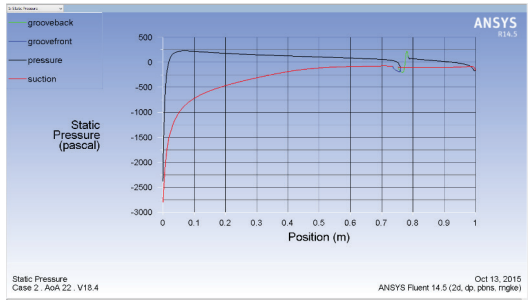

Figure 8: Case Two static pressure

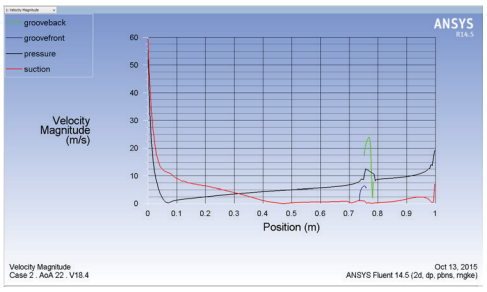

Figure (9). Velocity magnitude curve

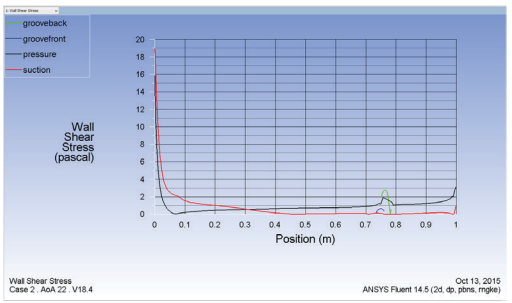

Figure (10). Wall shear stress

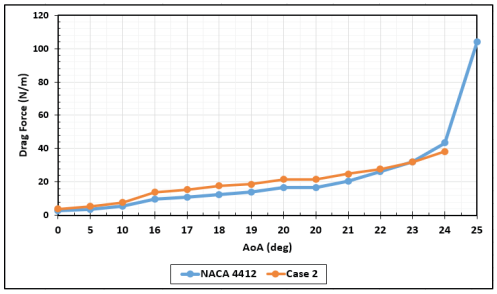

Figure (11). Comparison of drag force between Case Two and NACA 4412 at approaching wind velocity 18.4 m/s.

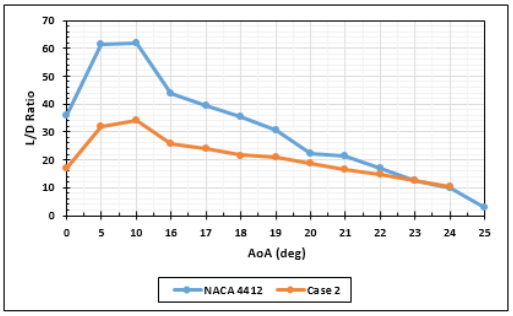

Figure (12). Comparison of lift/drag ratio between Case Two and NACA 4412 at approaching wind velocity 18.4 m/s.

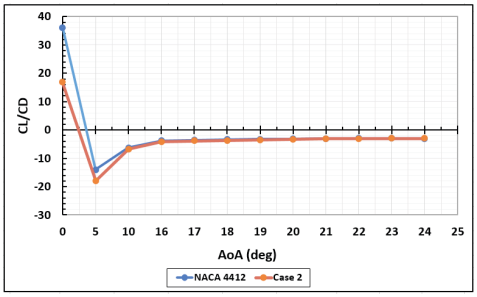

Figure (13). Comparison of (C_L/C_D) Ratio Variation Between the Original NACA4412 and Case 2

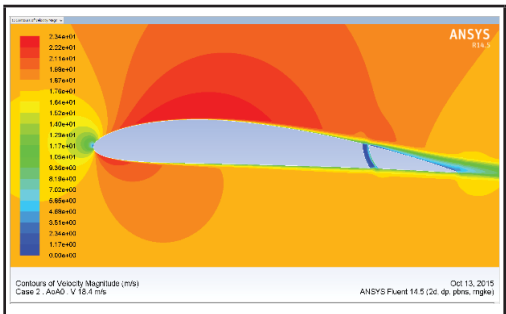

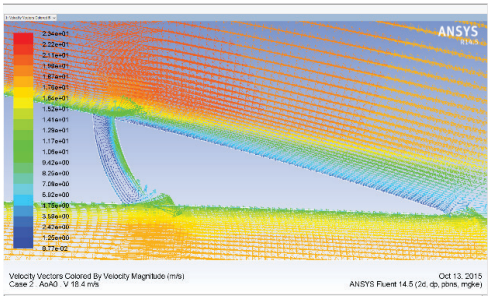

Velocity magnitude vectors across the groove

Figure A: Velocity Magnitude at AoA0 and 18.4 m/s

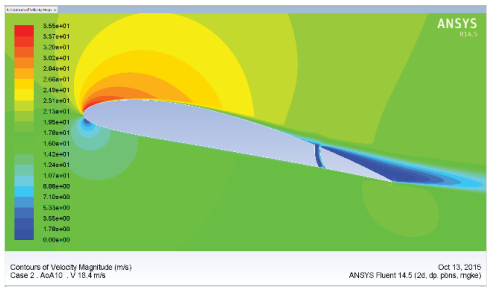

Velocity magitude contours

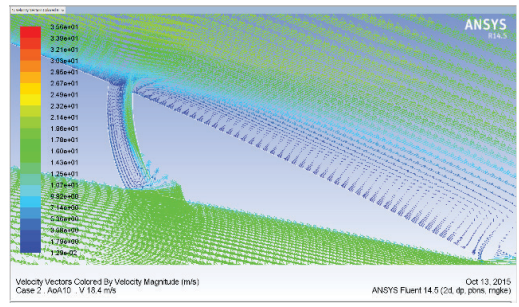

Velocity magnitude vectors across the groove

Figure B: Velocity magnitude at AoA10 and 18.4 m/s

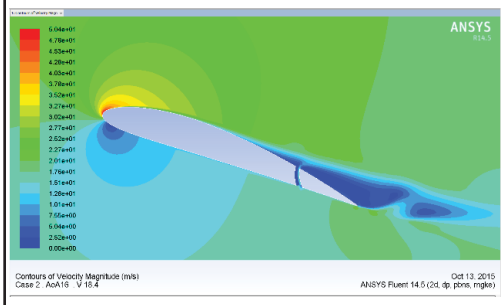

Velocity magitude contours

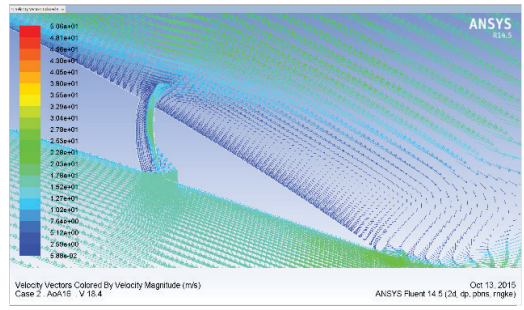

Velocity magnitude vectors across the groove

Figure C: Velocity at AoA16 and 18.4 m/s

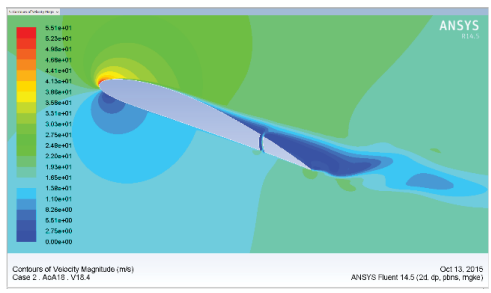

Velocity magnitude contours

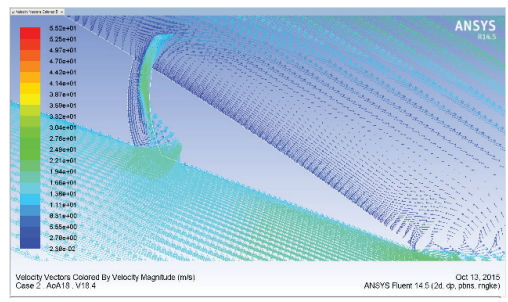

Velocity magnitude vectors across the groove

Figure D: Velocity at AoA18 and 18.4 m/s

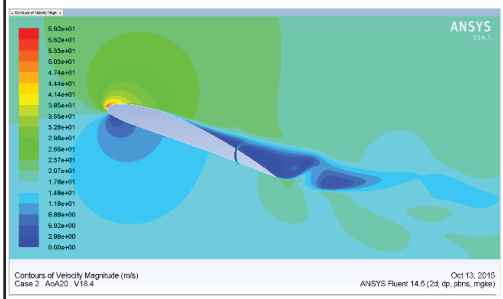

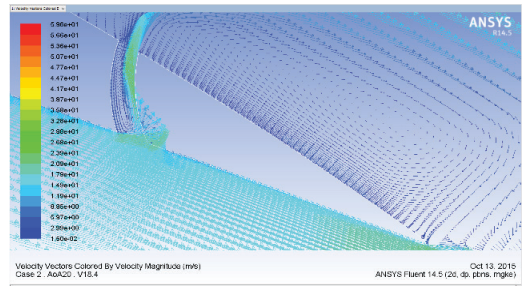

Figure E: Velocity at AoA20 and 18.4 m/s

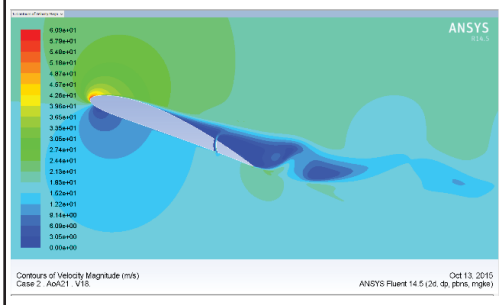

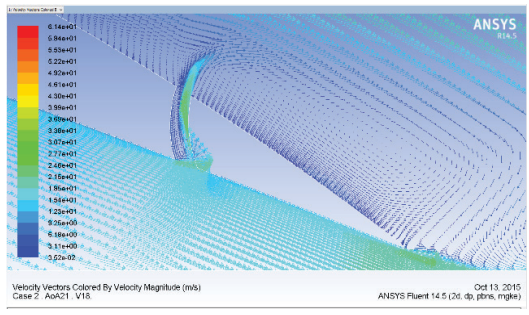

Velocity magitude contours	Velocity magnitude vectors across the groove

Figure F: Velocity at AoA21 and 18.4 m/s

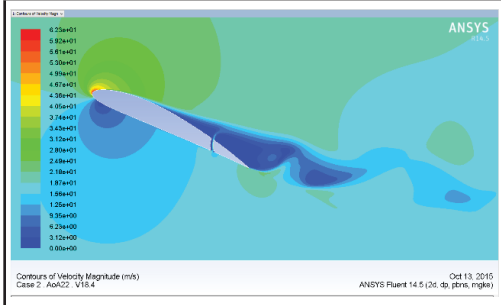

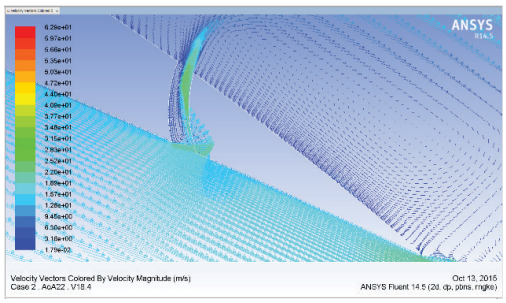

Velocity magitude contours	Velocity magnitude vectors across the groove

Figure G: Velocity at AoA22 and 18.4 m/s

Figure 14: Velocity magnitude at different angles of attack and wind velocity of 18.4 m/s

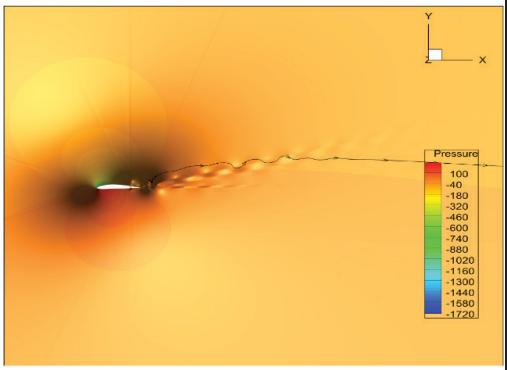

Figure (15).Formation of turbulences

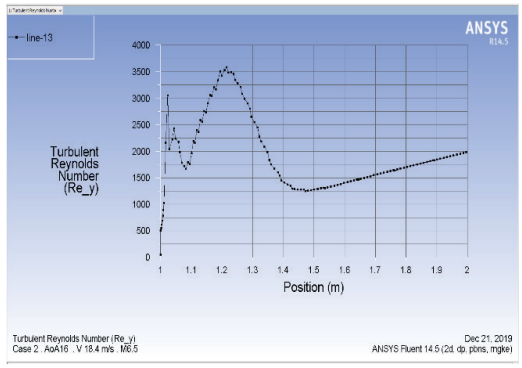

Figure (16). Variation of Turbulent Reynolds Number at the Domain Outlet

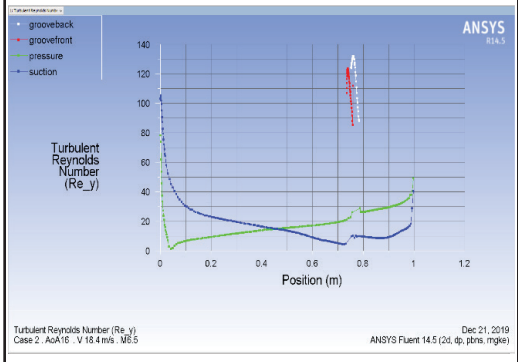

Figure (17). Variation of Turbulent Reynolds Number Along the airfoil body

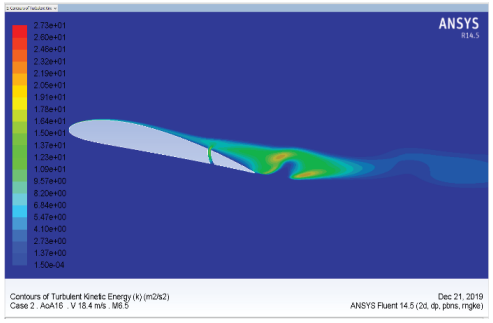

Figure (18).Contours of Turbulent Kinetic Energy Along the Airfoil Body

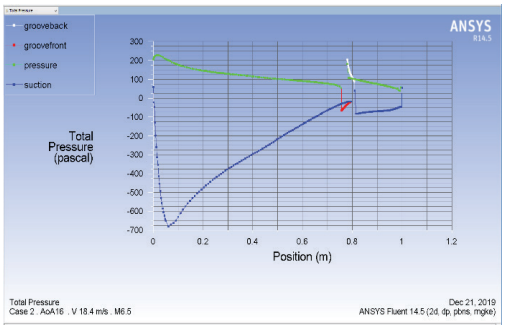

Figure (19). Total Pressure

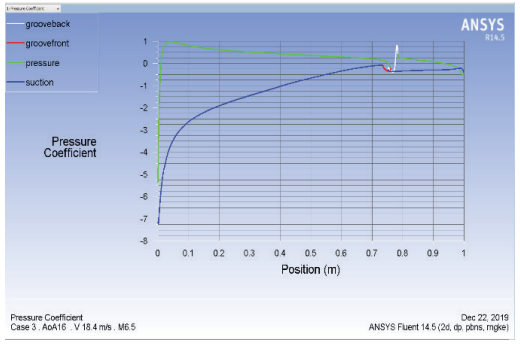

Figure (20).Pressure Coefficient

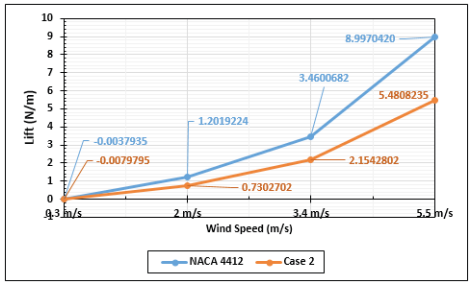

Figure (21). Comaprison of lift force between NACA 4412 and Case Two at Low wind speeds and AoA0

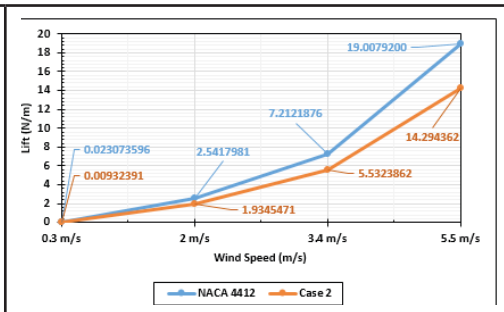

Figure (22). Comaprison of lift force between NACA 4412 and Case Two at low wind speeds and AoA5

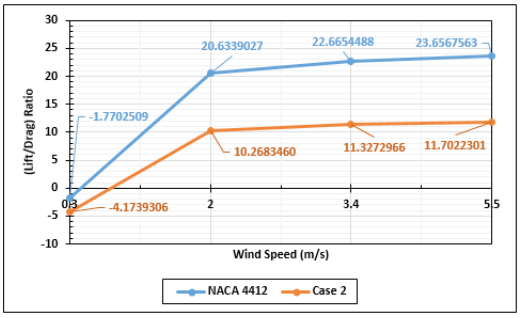

Figure (23). Comaprison of lift /drag ratio between NACA 4412 and Case Two at low wind speeds and AoA0

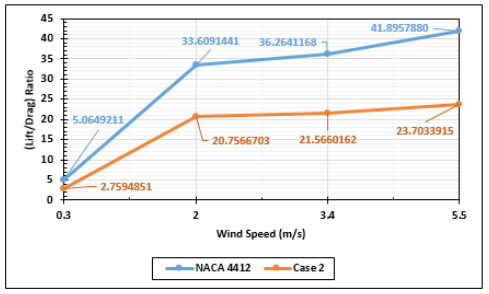

Figure (24). Comaprison of lift force between NACA 4412 and Case Two at low wind speeds and AoA5

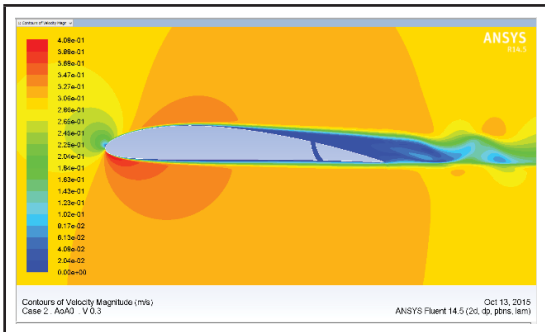

Velocity magnitude contours

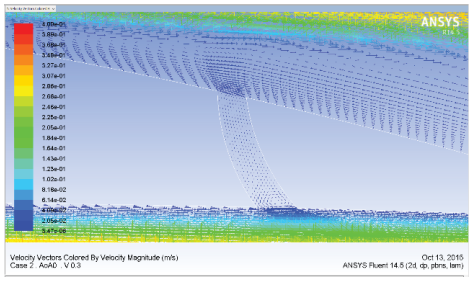

Velocity magnitude vectors across the groove

Figure A:AoA0 and 0.3 m/s

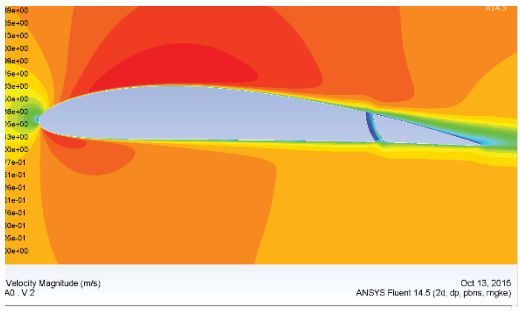

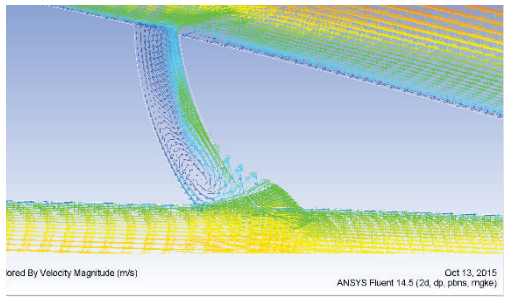

Velocity magitude contours	Velocity magnitude vectors across the groove

Figure B:AoA0 and 2 m/s

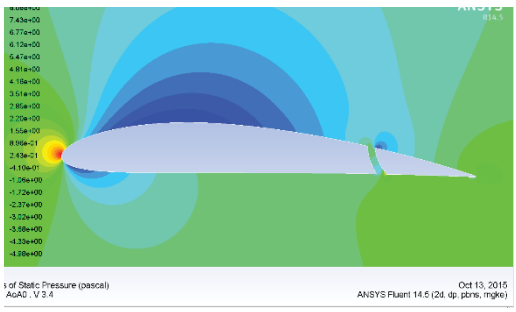

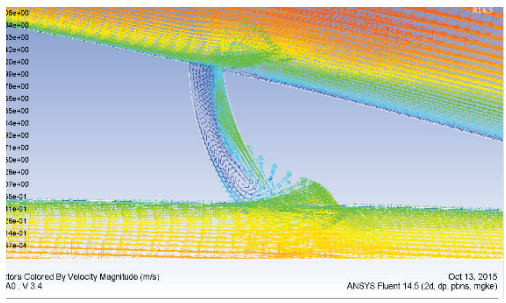

Velocity magitude contours	Velocity magnitude vectors across the groove

Figure C:AoA0 and 3.4 m/s

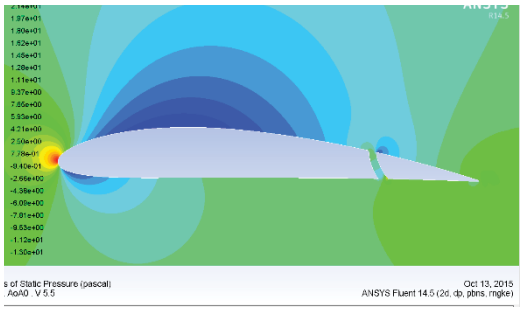

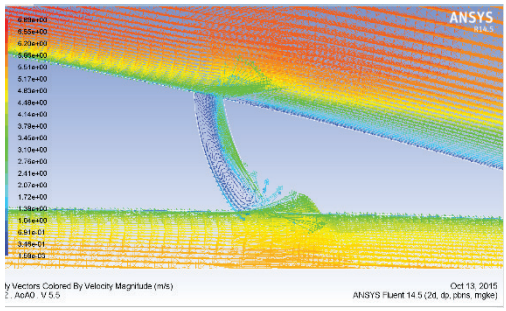

Velocity magitude contours	Velocity magnitude vectors across the groove

Figure D:AoA0 and 5.5 m/s

Figure (25). Velocity at AoA0 and low approaching wind velocity